PHYSICAL REVIEW A **87**, 061802(R) (2013)

Theory of electromagnetically induced transparency in strongly correlated quantum gases

H. H. Jen[1] and Daw-Wei Wang[1,2]

[1]*Physics Department, National Tsing Hua University, Hsinchu, Taiwan, Republic of China*

[2]*Physics Division, National Center for Theoretical Sciences, Hsinchu, Taiwan, Republic of China*

(Received 19 March 2013; published 13 June 2013)

We develop a general theory to study the electromagnetically induced transparency (EIT) in ultracold quantum gases, applicable for both Bose and Fermi gases with an arbitrary interparticle interaction strength. We show that, in the weak probe field limit, the EIT spectrum is solely determined by the single-particle Green's function of the ground-state atoms, and reflects interesting quantum many-body effects when atoms are virtually coupled to the low-lying Rydberg states. As an example, we apply our theory to a one-dimensional Luttinger liquid, a Bose-Mott insulator state, and the superfluid state of two-component Fermi gases, and show how the many-body features can be observed nondestructively in the unconventional EIT spectrum.

DOI: 10.1103/PhysRevA.87.061802 PACS number(s): 42.50.Gy, 67.85.−d, 71.10.Pm

Introduction. In the past decade, systems of ultracold atoms have opened up great opportunities to study many-body physics, which may not even exist in traditional condensed-matter systems [1]. Huge advances in the experimental techniques of tuning interaction strengths and generating an optical lattice enable the study of strongly correlated atomic gases with high controllability. Most of the experimental measurements rely on the interference pattern of the matter wave in different circumstances, for example, the time-of-flight experiment, the noise correlation measurement [2], and the Bragg scattering spectroscopy [3], etc. *In situ* imaging is also shown to be important in characterizing the equation of state and the critical properties near the phase transition point [4,5].

Besides the many-body problem, the quantum control and manipulation of the light-atom interaction is also an extensively studied field in cold atoms. One of the most important examples is electromagnetically induced transparency (EIT), which has led to several interesting subjects, such as the dark-state polariton, slow light, and the induced photon-photon interaction in a cold atomic gas [6,7]. EIT experiments in quantum degenerate gases [8,9] or in Rydberg states [10–13] are also recently explored by several groups. However, so far the EIT theory is still mainly based on the single-particle picture (or within a mean-field approximation), and therefore cannot clarify the nontrivial coupling between the light-atom interaction and the many-body physics. For example, how is the EIT spectrum modified when the ground state is a strongly correlated state without single-particle excitations? In what conditions can a nontrivial many-body effect be measured experimentally? Resolving these interdisciplinary problems is not only an interesting theoretical subject itself, but may be also applied to experimentally detect some many-body properties via EIT spectroscopy.

In this Rapid Communication, we develop a general EIT theory in a strongly interacting quantum gas, taking into account the full kinetics and interatomic interaction, within the weak probe field limit. We explicitly show how the experimental EIT spectrum is directly related to the dynamical Green's function, and how the quantum many-body phenomena are manifested most when atoms are coupled to a low-lying Rydberg state due to sufficient recoil energy compared to the decay rate of the excited state [14]. As an example, we apply our theory to three important strongly correlated systems: a Luttinger liquid of one-dimensional (1D) Bose gases, a Bose-Mott insulator in an optical lattice, and the superfluid state of two-component Fermi gases. For the Luttinger liquid, we demonstrate a power-law dependence of the EIT spectrum near the resonance, while the significant frequency shift and the asymmetric absorption spectrum can be identified for the other cases. Our results demonstrate the strongly correlated effects in the EIT experiment, suggesting a nondestructive measurement on the quantum gases.

General EIT theory for quantum gases. We consider the conventional EIT setup (Λ-type scheme) as shown in Fig. 1(a): Atoms are initially prepared in the ground state $|g\rangle$. The probe (Ω_1) and control (Ω_2) fields couple the ground state to another low-energy state $|s\rangle$ and an excited state $|e\rangle$ with detunings $\Delta_1 = \omega_1 - (E_e - E_g)$ and $\Delta_2 = \omega_2 - (E_e - E_s)$, respectively, where we set $\hbar = 1$. Here $\omega_{1,2}$ are central frequencies of probe and control fields, while $E_{g,s,e}$ denote the energies of atoms in different internal states. After using the dipole approximation and rotating wave approximation, the total Hamiltonian [$\hat{H}_{\rm tot} = \hat{H}_0 + \hat{H}_U + \hat{H}_1(t)$] in the rotating frame becomes

$$\begin{aligned}\hat{H}_0 &= \sum_{c=\{g,s,e\}}\sum_{\mathbf{k}}\left(\frac{\mathbf{k}^2}{2m}-\mu\right)\hat{c}^\dagger_{\mathbf{k}}\hat{c}_{\mathbf{k}} \\ &\quad+\sum_{\mathbf{k}}\left[(\Delta_2-\Delta_1)\hat{s}^\dagger_{\mathbf{k}}\hat{s}_{\mathbf{k}}-\Delta_1\hat{e}^\dagger_{\mathbf{k}}\hat{e}_{\mathbf{k}}\right] \\ &\quad-\sum_{\mathbf{k}}\left(\Omega_2\hat{e}^\dagger_{\mathbf{k}+\mathbf{k}_1}\hat{s}_{\mathbf{k}+\mathbf{k}_1-\mathbf{k}_2}+\text{H.c.}\right), \qquad (1)\\ \hat{H}_U &= \frac{1}{2V}\sum_{c,d=\{g,s,e\}}\sum_{\mathbf{k},\mathbf{k}',\mathbf{q}}U_{cd}\,\hat{c}^\dagger_{\mathbf{k}+\mathbf{q}}\hat{d}^\dagger_{\mathbf{k}'-\mathbf{q}}\hat{d}_{\mathbf{k}'}\hat{c}_{\mathbf{k}}, \\ \hat{H}_1(t) &= -\frac{1}{V}\sum_{\mathbf{k},\mathbf{q}}\bar{\Omega}_{1,\mathbf{k}}(t)\hat{e}^\dagger_{\mathbf{k}+\mathbf{q}}\hat{g}_{\mathbf{q}}+\text{H.c.}.\end{aligned}$$

Here $\hat{c}_{\mathbf{k}}$ and/or $\hat{d}_{\mathbf{k}}$ denote the atomic field operators in the momentum space. $\hat{H}_0$ includes all the single-particle parts without the probe field for atomic mass m, chemical potential μ, and the Rabi frequency of plane-wave control field Ω_2. All the interatomic interactions are included in $\hat{H}_U$ with the

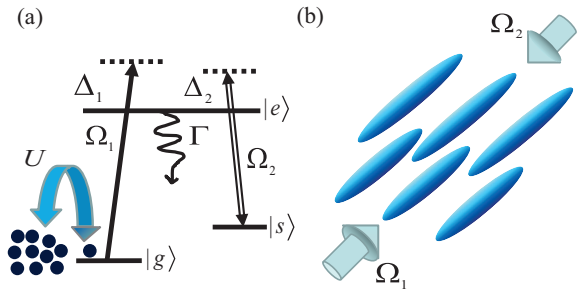

FIG. 1. (Color online) (a) Schematic figure of a standard EIT experiment in a strongly interacting atomic gas with the Λ-type scheme: The control (Ω_2) and the probe (Ω_1) fields couple two hyperfine ground states $|g\rangle$ and $|s\rangle$ with the excited state $|e\rangle$ (detunings are Δ_2 and Δ_1, respectively). Γ is the spontaneous decay rate of $|e\rangle$. Solid circles denote atoms with mutual interaction U in the ground state. (b) Experimental setup for EIT on a two-dimensional (2D) array of 1D Luttinger liquids in the counterpropagating scheme.

short-range interaction U_{cd} (extension to a certain long-ranged interaction is straightforward). Finally, $\hat{H}_1$ denotes the effect of the probe field with $\bar{\Omega}_{1,\mathbf{k}}(t)$ being the slowly varying Rabi frequency of wave vector $\mathbf{k}$. V is the quantization volume and $\mathbf{k}_{1,2}$ are momenta of the probe and control fields, respectively.

To derive the electric susceptibility in the linear response of the probe field [7], we treat H_1 as a time-dependent perturbation and keep the full interaction effects. Therefore, $\hat{H} \equiv \hat{H}_0 + \hat{H}_U$ can be separated into two decoupled parts, $\hat{H} = \hat{H}^g + \hat{H}^{se}$, where $\hat{H}^g$ includes all the ground-state kinetic energy and interaction energy terms, while $\hat{H}^{se}$ includes all the single-particle terms of states $|s\rangle$ and $|e\rangle$ (see Supplemental Material (SM) [16]). In the leading-order limit of a weak probe, all atoms are in the ground state ($|g\rangle$) and none in states $|e\rangle$ and $|s\rangle$. As a result, the interaction between $|g\rangle$ and the other two states is nothing but a background energy shift in the single-particle energy, i.e., $E_{s/e} \to E_{s/e} + nU_{g,s/e}$, where n is the total particle density. The mutual interaction between $|s\rangle$ and $|e\rangle$ is the second-order effect and is hence negligible. A similar treatment can be also easily applied to a long-ranged interaction if Rydberg states of a high principal quantum number are involved [17].

A phenomenological spontaneous decay rate (Γ) of the excited state can be added, and we also assume a negligible dephasing rate between the two hyperfine ground states. Note that when considering a standard $D2$ transition, $\Gamma \approx 6$ MHz, which is much larger than the average atomic kinetic energy, and therefore the quantum many-body effect may not be easily observed.

Defining the polarization operator, $\hat{P}(\mathbf{r},t) = d_0[\hat{\psi}_e^\dagger(\mathbf{r},t)\hat{\psi}_g(\mathbf{r},t) + \text{H.c.}]$, where $\hat{\psi}_{g/e}^\dagger(\mathbf{r},t)$ is the field operator, and d_0 is the dipole moment, we calculate its variation with respect to the probe field (H_1) via the linear response theory [23], $\delta\langle\hat{P}(\mathbf{r},t)\rangle = i\int_{-\infty}^{t} dt' {}_H\langle\Psi_G|[\hat{H}_{1,H}(t'),\hat{P}_H(\mathbf{r},t)]|\Psi_G\rangle_H$, where $\hat{H}_{1,H}(t)$ and $\hat{P}_H(\mathbf{r},t)$ are the corresponding operators in the Heisenberg picture, and $|\Psi_G\rangle_H$ is the ground state of the unperturbed Hamiltonian $\hat{H} = \hat{H}^g + \hat{H}^{se}$. In the momentum-frequency space, the electric susceptibility can be obtained to be (see SM [16])

$$\chi(\mathbf{q},\omega) = -\frac{d_0}{V}\sum_{\mathbf{k}}\int_{-\infty}^{\infty} d\tilde{\omega} i\tilde{G}^<(\mathbf{k},\tilde{\omega}) \times\left[\frac{\cos^2\phi_{\mathbf{k}+\mathbf{q}}}{\tilde{\omega}-\omega-\epsilon_-(\mathbf{k}+\mathbf{q})} + \frac{\sin^2\phi_{\mathbf{k}+\mathbf{q}}}{\tilde{\omega}-\omega-\epsilon_+(\mathbf{k}+\mathbf{q})}\right]. \quad (2)$$

Here $\tilde{G}^<(\mathbf{k},\tilde{\omega})$ is the Fourier transform of the Green's function at zero temperature [23], $G^<(0,0;\mathbf{r},t) \equiv \mp i\,{}_H\langle\Psi_G|\hat{\psi}_g^\dagger(\mathbf{r},t)\hat{\psi}_g(0,0)|\Psi_G\rangle_H\theta(t)$, where the upper (lower) sign refers to bosons (fermions). We note that the above result is very general in the limit of the weak probe field, and all the many-body effects are hidden in $\tilde{G}^<(\mathbf{k},\tilde{\omega})$. However, as pointed out in Ref. [24], such a many-body effect can be identified more easily in the counterpropagating (rather than the copropagating) setup of the EIT experiment, since the recoil momentum of the former is manifested more significantly in the quantum statistics. In the rest of this Rapid Communication, therefore, we just consider the counterpropagating scheme in order to measure the many-body effect from the EIT spectrum.

EIT in Luttinger liquid. Now we study EIT in a Luttinger liquid (LL), as shown in Fig. 1(b), which is a very general 1D effective model [25,26] and has no condensate even at zero temperature. Since all the elementary excitations of a LL are collective, it is therefore interesting to investigate how the probe field propagates inside such a strongly correlated system. The single-particle Green's function can be exactly calculated by the bosonization method [26] (see SM [16]),

$$iG_{\text{LL}}^<(x,t) = \frac{na^{1/2\kappa}}{[x^2+(a+ivt)^2]^{1/4\kappa}}, \quad (3)$$

where κ is the Luttinger parameter, v is the phonon velocity, and a^{-1} is the system-dependent momentum cutoff. $1 < \kappa < \infty$ for a short-ranged repulsive interaction, while κ can be smaller than one if the interaction is long ranged.

In Figs. 2(a) and 2(b), we show the full numerically integrated EIT absorption and dispersion profiles [from Eqs. (2) and (3)] of 1D ^{87}Rb atoms (see the caption for the parameters) in the counterpropagating scheme. It is easy to see that the power-law dependence of χ_{LL} makes the dispersion highly asymmetric about the resonance points and the absorption depth (α) becomes larger at the transparency point (Δ_1^*) in the strong interacting regime (smaller κ), in contrast to the standard EIT profiles in the weak interacting limit ($\kappa \gg 1$). This is because when a ground-state atom is excited by the probe field, the transition matrix elements are a composite of all the collective excitations of different energies, weighted by the density of states in a power-law distribution. In Fig. 2(c), we show the group velocity of light (proportional to the slope of dispersion at the transparent point, where the absorption is the smallest) as a function of κ. One can see that for a stronger interaction (smaller κ), the group velocity becomes smaller due to steeper dispersion relations, but the absorption is also larger, making the slow light propagate less effectively in a LL. On the other hand, such an unconventional EIT spectrum also implies a sensitive measurement about the many-body properties.

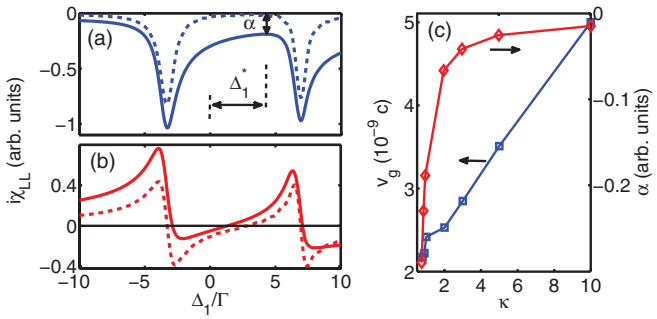

FIG. 2. (Color online) The EIT profiles for a Luttinger liquid of ^{87}Rb atoms in the counterpropagating excitation scheme. We take a static probe field ($\mathbf{q},\omega = 0$) and a resonant control field ($\Delta_2 = 0$) with Rabi frequency $\Omega_2 = 5\Gamma$. The excited state is chosen as a low-lying Rydberg transition of $|24P_{3/2}\rangle$ with the spontaneous decay rate $\Gamma^{-1} = 28.3\ \mu$s. The effective 1D interaction strength can be tuned by the confinement resonance of 1D tubes [27]. (a) Absorption (Re[$i\chi$]) and (b) dispersion (Im[$i\chi$]) profiles for $\kappa = 1$ (solid) and 10 (dashed). The horizontal line guides the eye to the zero in (b). (c) shows the group velocity v_g (□), and the absorption depth α (◇) at the transparency point (Δ_1^*) as a function of κ. For convenience, we take the phonon velocity $v = 4.3$ mm/s and the cutoff $a = 0.12\ \mu$m within a typical experimental regime [28]. c is the speed of light.

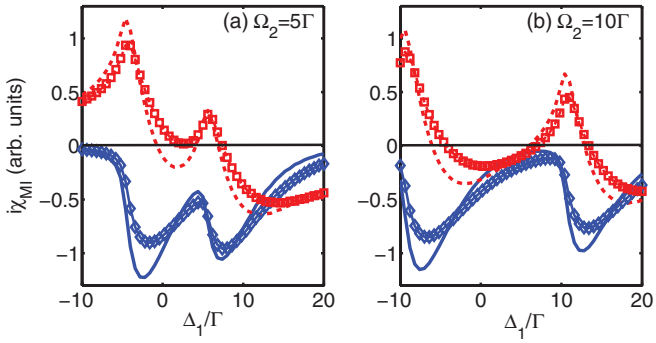

FIG. 3. (Color online) EIT profiles of a unit-filling Mott insulator with ^{87}Rb atoms loaded in a 3D optical lattice (lattice constant $d =$ 426 nm). The corresponding parameters (U,J) in units of the recoil energy E_R are (0.5,0.007) and (1.05,10^{-4}) for $V_0/E_R = 15$ (solid blue and dashed red) and 40 (◇ and □), respectively. Absorption (Re[$i\chi$], solid blue, ◇) and dispersion (Im[$i\chi$], dashed red, □) profiles are plotted for various control field strengths (a) $\Omega_2 = 5$ and (b) 10Γ. All other parameters are the same as in Fig. 2.

EIT in a Mott insulator. Now we consider the Mott insulator (MI) of strongly interacting bosons in a three-dimensional (3D) optical lattice, which can be well described by a single-band Hubbard model (HM) [29]. The ground-state field operator is expressed as $\hat{\psi}_g(\mathbf{r},t) = \sum_{\mathbf{R}} \hat{g}_{\mathbf{R}}(t) w_{\mathbf{R}}(\mathbf{r})$, where $w_{\mathbf{R}}(\mathbf{r})$ is the Wannier function, and $\hat{g}_{\mathbf{R}}(t)$ is the field operator at site $\mathbf{R}$. When deep inside the MI state, we can use the three-state model [30,31] to control the small number fluctuation above the Fock state, and obtain the Green's function at zero temperature (see SM [16]), $i\tilde{G}^<(\mathbf{k},t) = n_0 \sum_{\mathbf{R}} |\tilde{w}_{\mathbf{R}}(\mathbf{k})|^2 e^{-i\epsilon_h(\mathbf{k})t}\theta(t)$, where n_0 is the integer filling fraction, $\tilde{w}_{\mathbf{R}}(\mathbf{k})$ is the Fourier transform of $w_{\mathbf{R}}(\mathbf{r})$, and $\epsilon_h(\mathbf{k}) = \epsilon_0(\mathbf{k})/2 + \delta\mu + \tilde{\omega}(\mathbf{k})$ is the hole excitation with $\tilde{\omega}(\mathbf{k}) \approx U/2$ when deep inside the Mott state. Here $\epsilon_0(\mathbf{k}) \equiv 2J\sum_{\alpha=1}^{3}\cos(\mathbf{k}_\alpha d)$, and $\delta\mu = -3J$ for a 3D square lattice of lattice constant d. J and U are the tunneling amplitude and on-site interaction. As a result, the susceptibility from Eq. (2) becomes

$$\chi_{\mathrm{MI}}(\mathbf{q},\omega) = \frac{d_0 N}{V}\sum_{\mathbf{k}} |\tilde{w}_{\mathbf{R}}(\mathbf{k})|^2 \left[\frac{\cos^2\phi_{\mathbf{k}+\mathbf{q}}}{\omega + \epsilon_h(\mathbf{k}) + \epsilon_-(\mathbf{k}+\mathbf{q})} + \frac{\sin^2\phi_{\mathbf{k}+\mathbf{q}}}{\omega + \epsilon_h(\mathbf{k}) + \epsilon_+(\mathbf{k}+\mathbf{q})}\right]. \quad (4)$$

Compared to the standard EIT spectrum, we find that χ_{MI} is contributed by EIT in different momentum states, weighting by the Wannier function of the optical lattice. When the momentum distribution is large in a strong lattice strength, the contribution from different momenta makes the EIT spectrum much broadened, in contrast to the superfluid state which is similar to the standard EIT spectrum in a Bose-Einstein condensate (BEC) [24].

In Fig. 3, we demonstrate the EIT spectrum inside the MI state of ^{87}Rb with unit filling for different control fields and lattice strengths. As discussed above, the momentum distribution of the Wannier function leads to an asymmetric and inhomogeneous broadening of the absorption profiles near the resonance. It makes the EIT window less transparent when the control field is weak [Fig. 3(a)], while it becomes less effective in the large field limit. In other words, by measuring the absorption depth, one may also determine the momentum distribution of the underlying many-body system.

EIT in a BCS superfluid state. Finally we investigate the EIT in a BCS superfluid of two-component Fermi gases, using a similar setup [15] by coupling one of the atomic ground states to a low-lying Rydberg state [14]. Without losing generality, here we just presume the existence of a superconducting gap Δ_{BCS}, not specifying the pairing mechanism. One of the two components (pseudo-spin-up) is our ground state ($|g\rangle$) in the EIT experiment, and the other is not involved in the EIT process. The Green's function can be calculated by transforming toward the Bogoliubov quasiparticles (α and β), $\hat{g}_{\mathbf{k},\uparrow} = \cos\theta_{\mathbf{k}}\hat{\alpha}_{\mathbf{k}} + \sin\theta_{\mathbf{k}}\hat{\beta}^\dagger_{-\mathbf{k}}$, where $\sin^2\theta_{\mathbf{k}} \equiv (1 - \xi_{\mathbf{k}}/E_{\mathbf{k}})/2$. Here $E_{\mathbf{k}} = \sqrt{\Delta_{\mathrm{BCS}}^2 + \xi_{\mathbf{k}}^2}$ is the excitation energy with $\xi_k \equiv \mathbf{k}^2/(2m) - \mu$ and μ being the chemical potential. We find that $-i\tilde{G}^<_{\mathrm{BCS}}(\mathbf{k},t) = \sin^2\theta_{\mathbf{k}}^2 e^{-iE_{\mathbf{k}}t}\theta(t)$ (see SM [16]), and then

$$\chi_{\mathrm{BCS}}(\mathbf{q},\omega) = \frac{d_0}{V}\sum_{\mathbf{k}} \sin^2\theta_{\mathbf{k}}\left(\frac{\cos^2\phi_{\mathbf{k}+\mathbf{q}}}{\omega + E_{\mathbf{k}} + \epsilon_-(\mathbf{k}+\mathbf{q})} + \frac{\sin^2\phi_{\mathbf{k}+\mathbf{q}}}{\omega + E_{\mathbf{k}} + \epsilon_+(\mathbf{k}+\mathbf{q})}\right). \quad (5)$$

Note that in the limit of zero pairing gap, $\Delta_{\mathrm{BCS}} = 0$, $\sin^2\theta_{\mathbf{k}}$ becomes a step function at the Fermi energy, and hence χ_{BCS} becomes the result of a noninteracting Fermi gas [24].

In Figs. 4(a) and 4(b), we plot the EIT profiles of the BCS superfluid phase for ^{40}K in the counterpropagating excitation schemes. Different control field strengths and different gap amplitudes are shown together for comparison. One can see that when the control field is turned smaller, the recoil energy becomes more important so that the presence of a Fermi sea makes the EIT spectrum disappear, similar to the noninteracting fermions [24]. When the control field

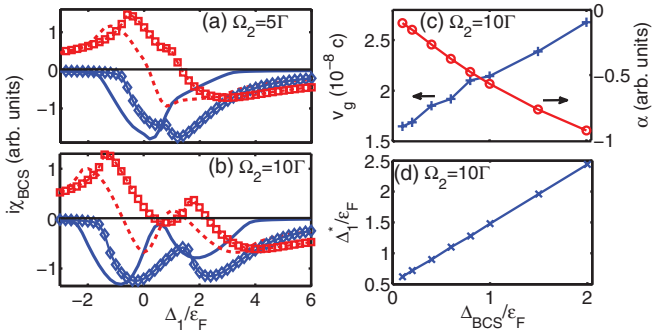

FIG. 4. (Color online) EIT profiles of a BCS superfluid state of two-component Fermi gases (^{40}K). The excited state is chosen as a low-lying Rydberg transition of $|21P_{3/2}\rangle$ with $\Gamma^{-1} = 25.4\ \mu$s. We fix the chemical potential $\mu = \epsilon_F = 6.7\hbar\Gamma$ with an atomic density $n \sim 10^{14}$ cm^{-3} and resonant control field ($\Delta_2 = 0$). Absorption (Re[$i\chi$], solid blue, ◊) and dispersion (Im[$i\chi$], dashed red, □) profiles are plotted for pairing gaps $\Delta_{\rm BCS}/\epsilon_F = 0.1$ (solid blue and dashed red) and 1 (◊ and □), while the control field strengths are (a) $\Omega_2 = 5$ and (b) 10Γ. (c) shows the group velocity v_g (+) and the absorption depth α (◯) at the transparency point as a function of $\Delta_{\rm BCS}$. (d) shows the transparency positions Δ_1^* (×).

becomes stronger, the quantum degeneracy becomes less important so that the standard EIT features appear, while an asymmetric broadening appears when the gap is opened. Interestingly, we find the group velocity is larger for a larger $\Delta_{\rm BCS}$ [see Fig. 4(c)], different from the results of a LL. In Fig. 4(d) we show that the transparency points Δ_1^* scale as the gap energy, and therefore can be used to measure the pairing gap.

Experimental issues. The difference between the EIT approach and standard Bragg spectroscopy (BS) is twofold. First, EIT is nondestructive while BS operates with the interference of atoms. Second, BS measures the density-density correlation function, in contrast to the first-order correlation in EIT. For experimental realizations, it may involve the integration time and precision of the spectrum measurement. With kHz resolution required in our scheme, we need a ms integration time compatible with the atomic lifetime of several ms, which can be fulfilled by minimizing the inelastic collisions of BEC [32]. The contrast of susceptibility can be also enhanced by increasing the optical depth of the atoms. Including the thermal excitations is crucial for practical implementations and will be discussed in a future work.

In summary, we have developed a general and analytical theory to investigate the EIT spectrum of quantum degenerate ultracold atoms. The spectrum is solely determined by the single-particle Green's function, and has most significant quantum many-body physics when the atoms are coupled to a low-lying Rydberg state. In the regime of strong interaction, the absorption profile has a highly asymmetric inhomogeneous broadening with a frequency shift in detuning. Our results suggest a new nondestructive method to investigate the strongly correlated physics from the well-developed EIT experiment.

Acknowledgments. We appreciate fruitful discussions with Ite A. Yu, Y.-C. Chen, M. Fleischhauer, and G. Juzeliūnas. This work is supported by NSC and NCTS grants in Taiwan.

[1] For a review, see, for example, I. Boch, J. Dalibard, and W. Zwerger, Rev. Mod. Phys. **80**, 885 (2008).
[2] E. Altman, E. Demler, and M. D. Lukin, Phys. Rev. A **70**, 013603 (2004).
[3] M. Kozuma *et al.*, Phys. Rev. Lett. **82**, 871 (1999); J. Stenger *et al.*, *ibid.* **82**, 4569 (1999); S. B. Papp *et al.*, *ibid.* **101**, 135301 (2008); G. Veeravalli, E. Kuhnle, P. Dyke, and C. J. Vale, *ibid.* **101**, 250403 (2008); J. M. Pino, R. J. Wild, P. Makotyn, D. S. Jin, and E. A. Cornell, Phys. Rev. A **83**, 033615 (2011).
[4] N. Gemelke, X. Zhang, C-L. Hung, and C. Chin, Nature (London) **460**, 995 (2009).
[5] T.-L. Ho and Q. Zhou, Nat. Phys. **6**, 131 (2010).
[6] M. D. Lukin, Rev. Mod. Phys. **75**, 457 (2003).
[7] M. Fleischhauer, A. Imamoglu, and J. P. Marangos, Rev. Mod. Phys. **77**, 633 (2005).
[8] L. V. Hau, S. E. Harris, Z. Dutton, and C. H. Behroozi, Nature (London) **397**, 594 (1999).
[9] U. Schnorrberger, J. D. Thompson, S. Trotzky, R. Pugatch, N. Davidson, S. Kuhr, and I. Bloch, Phys. Rev. Lett. **103**, 033003 (2009).
[10] M. Saffman and T. G. Waller, Rev. Mod. Phys. **82**, 2313 (2010).
[11] Y. O. Dudin and A. Kuzmich, Science **336**, 887 (2012).
[12] J. D. Pritchard, D. Maxwell, A. Gauguet, K. J. Weatherill, M. P. A. Jones, and C. S. Adams, Phys. Rev. Lett. **105**, 193603 (2010).
[13] T. Peyronel, O. Firstenberg, Q. Liang, S. Hofferberth, A. V. Gorshkov, T. Pohl, M. D. Lukin, and V. Vuletic, Nature (London) **488**, 57 (2012).
[14] In the EIT theory developed by Jiang *et al.* [15] for a Fermi pairing gas, they consider a standard $D2$ transition where the recoil energy is smaller than the decay rate of the excited state. In order to observe a quantum many-body effect in such a setup, the control field (Ω_2) has to be tuned much smaller than the decay rate (Γ), making it more difficult to be experimentally observed.
[15] L. Jiang, H. Pu, W. Zhang, and H. Y. Ling, Phys. Rev. A **80**, 033606 (2009).
[16] See Supplemental Material at http://link.aps.org/supplemental/10.1103/PhysRevA.87.061802 for detailed derivations of the linear susceptibility and single-particle Green's function.
[17] In this Rapid Communication, we just consider low-lying Rydberg states ($n'P$ levels, $n' < 30$) [18,19] of alkali atoms. The van der Waals coefficient $|C_6|$ for $30P$–$30P$ rubidium asymptotes is in the range of (0.26–4.7) × 10^{16} a.u. [20], giving us the blockade radius $R_c = 0.88-1.29\ \mu$m [21,22] for a density $n = 10^{14}$cm^{-3} with the effective excitation Rabi frequency $\Omega_1 = 2\pi \times 100$ kHz. This radius provides an upper estimation of the dipole blockade strength, which can be further reduced by decreasing Ω_1. Note that the probe field has a fundamental limit of single-photon shot noise which can be overcome by more

experimental trials. As a result, we neglect the blockade in our theory.

[18] T. F. Gallagher, *Rydberg Atoms* (Cambridge University Press, Cambridge, UK, 1994).

[19] D. Tong, S. M. Farooqi, J. Stanojevic, S. Krishnan, Y. P. Zhang, R. Côté, E. E. Eyler, and P. L. Gould, Phys. Rev. Lett. **93**, 063001 (2004).

[20] K. Singer, J. Stanojevic, M. Weidemüller, and R. Côté, J. Phys. B: At. Mol. Opt. Phys. **38**, S295 (2005).

[21] R. Löw, H. Weimer, U. Krohn, R. Heidemann, V. Bendkowsky, B. Butscher, H. P. Büchler, and T. Pfau, Phys. Rev. A **80**, 033422 (2009).

[22] R. Heidemann, U. Raitzsch, V. Bendkowsky, B. Butscher, R. Löw, L. Santos, and T. Pfau, Phys. Rev. Lett. **99**, 163601 (2007).

[23] A. L. Fetter and J. D. Walecka, *Quantum Theory of Many-Particle Systems* (Dover, New York, 2003).

[24] H. H. Jen, B. Xiong, I. A. Yu, and D.-W. Wang, arXiv:1208.0118.

[25] F. D. M. Haldane, Phys. Rev. Lett. **47**, 1840 (1981); J. Phys. C: Solid State Phys. **14**, 2585 (1981).

[26] M. A. Cazalilla, J. Phys. B: At. Mol. Opt. Phys. **37**, S1 (2004).

[27] M. Olshanii, Phys. Rev. Lett. **81**, 938 (1998).

[28] T. Kinoshita, T. Wenger, and D. S. Weiss, Science **305**, 1125 (2004).

[29] M. P. A. Fisher, P. B. Weichman, G. Grinstein, and D. S. Fisher, Phys. Rev. B **40**, 546 (1989).

[30] D.-W. Wang, Phys. Rev. A **80**, 063620 (2009).

[31] E. Altman and A. Auerbach, Phys. Rev. Lett. **89**, 250404 (2002).

[32] R. Zhang, S. R. Garner, and L. V. Hau, Phys. Rev. Lett. **103**, 233602 (2009).